Available online at www.sciencedirect.com
SCIENCE DIRECT®
International Journal of Thermal Sciences 42 (2003) 1061–1071
International Journal of Thermal Sciences
www.elsevier.com/locate/ijts

Optimized use of baffles for reduced natural convection heat transfer from a horizontal cylinder

Bassam A/K Abu-Hijleh

School of Aerospace, Mechanical and Manufacturing Engineering, RMIT University, Bundoora East Campus, P.O. Box 71, Bundoora, 3083 Victoria, Australia

Received 21 October 2002; accepted 7 March 2003

Abstract

The problem of laminar natural convection from a horizontal cylinder with one or more low conductivity fins (baffles) on its outer surface was investigated numerically. The aim was to optimize the number, size, and location of the baffle(s) for maximum natural convection heat convection, i.e., Nusselt number, over a wide range of Rayleigh number. The percentage reduction in heat transfer per baffle(s) unit length "cost-efficiency" was also studied. Changes in the thermodynamic efficiency was studied by calculating the entropy generation associated with each baffle configuration. It was found that the proper placement of a single or dual baffles has a significant effect on the heat transfer and entropy generatuion reduction. The optimal single and dual baffle locations is reported for different values of Rayleigh number and baffle height.

1. Introduction

Laminar convection from a heated cylinder is an important problem in heat transfer. It is used to simulate a wide range of engineering applications as well as provide a better insight into more complex systems of heat transfer. Accurate knowledge of the overall natural convection heat transfer around circular cylinders is important in many fields, including heat exchangers, hot water and steam pipes, heaters, refrigerators and electrical conductors. Because of its industrial importance, this class of heat transfer has been the subject of many experimental and analytical studies. The problem received continuous attention since the early work of Morgan [1] and Churchill and Chu [2]. The most widely referenced work in this area is that of Kuehn and Goldstein [3] which included the first numerical solution of the full elliptic governing equations. Although more recent work and more accurate work has been reported in the literature since then [4–6] the work of Kuehn and Goldstein [3] is still being referenced [7,8]. Recent economic and environmental concerns have raised the interest in methods of reducing or increasing the natural heat transfer, depending on the application, from a horizontal cylinder. Classical methods such as the use of insulation materials are becoming a cost as well as an environmental concern. Researchers continue to look for new methods of heat transfer control. The use of porous material to alter the heat transfer characteristics has been reported by several researchers including Vafai and Huang [9] and Al-Nimr and Alkam [10]. The results of using uniformly spaced baffles to reduce natural heat transfer from a cylinder were recently published by the author [11].

Recently, entropy generation (or production) has been used to gauge the significance of irreversibility related to heat transfer, friction, and other non-ideal processes within thermal systems [12]. The rate of useful energy lost owing to irreversibility is proportional to the rate of entropy generation. Entropy-generation calculations can be used to optimize the thermodynamic behavior of thermal systems both on the component level and as complete systems. Knowledge of the locations and levels of high entropy generation will help focus the designers' efforts on the regions or components that contribute most to the irreversibility and thus inefficiency of the system [11,13].

This paper presents the numerical results of using low conductivity baffles on the cylinder's outer surface in order to suppress the natural convection currents around the cylinder, which should translate to a lower heat transfer rate. Different numbers of baffles were placed at different tangential location in order to find the optimal placement

E-mail address: bassam.abu-hijleh@rmit.edu.au (B. A/K Abu-Hijleh).

1290-0729/$ – see front matter
doi:10.1016/S1290-0729(03)00089-9

Nomenclature

B	number of baffles
D	cylinder diameter, $= 2r_o$ ..... m
E	parameter in computational domain, $= \pi e^{\pi\xi}$
g	gravity ..... $m{\cdot}s^{-2}$
H	non-dimensional baffle height, $= h_b/r_o$
h	local convection heat transfer coefficient ..... $W{\cdot}m^{-2}{\cdot}K^{-1}$
h_b	baffle height ..... m
k	conduction heat transfer coefficient ..... $W{\cdot}m^{-1}{\cdot}K^{-1}$
M	number of grid points in the tangential direction
N	number of grid points in the radial direction
N_s	total non-dimensional entropy generation
$Nu_{D,s}$	local Nusselt number based on cylinder diameter
$\overline{Nu_D}$	average Nusselt number based on cylinder diameter
$\overline{Nu_{D,B}}$	average Nusselt number based on cylinder diameter, cylinder with B baffles
P	non-dimensional pressure
p	pressure ..... Pa
Pr	Prandtl number
R	non-dimensional radius
r	radius ..... m
Ra	Rayleigh number based on cylinder radius, $= g\beta(T_o - T_\infty)r_o^3/\alpha\nu$
Ra_D	Rayleigh number based on cylinder diameter, $= g\beta(T_o - T_\infty)D^3/\alpha\nu$
S''_{gen}	non-dimensional local entropy generation
s''_{gen}	dimensional local entropy generation per unit depth, i.e., 2D ..... $W{\cdot}m^{-2}{\cdot}K^{-1}$
T	temperature ..... K
U	non-dimensional radial velocity
u	radial velocity ..... $m{\cdot}s^{-1}$
V	non-dimensional tangential velocity
v	tangential velocity ..... $m{\cdot}s^{-1}$

Greek symbols

α	thermal diffusivity ..... $m^2{\cdot}s^{-1}$
β	coefficient of thermal expansion ..... K^{-1}
ε	measure of convergence of numerical results
η	independent parameter in computational domain representing tangential direction
θ	angle (degree)
ν	kinematic viscosity ..... $m^2{\cdot}s^{-1}$
ξ	independent parameter in computational domain representing radial direction
ρ	density ..... $kg{\cdot}m^{-3}$
ϕ	non-dimensional temperature
ψ	stream function
ω	vorticity function

Subscripts

D	value based on cylinder diameter
o	value at cylinder surface
∞	free stream value

of the baffles. Constructal theory [14] suggests that there is an "optimal distribution of imperfection", i.e., the baffles in this case, that leads to global optimization of the system performance, i.e., natural convection heat transfer in the current case. The theory focuses on the degree(s) of freedom that a system contains based on geometric considerations. It is such a manipulation of the baffle(s) geometric degrees of freedom that this paper addresses in order to optimize the global thermal behavior of the cylinder under different thermal conditions.

The fluid under consideration is Air. The numerical solution of the elliptic momentum and energy equations was performed using the stream function-vorticity method on a stretched grid. The computed velocity and temperature fields were used to compute the local and global entropy generation. This detailed study included varying the Rayleigh number from 10^3 to 10^5, number of baffles from 0 to 11, the non-dimensional baffle height from 0.1 to 1.5, and the cylinder diameter from 10^{-3} to 10 meters. This range of values was based on the experience gained from a previous work using only uniformly spaced baffles [11]. Due to symmetry, the computations were carried on half the physical domain making use of the vertical symmetry plane passing through the center of the cylinder. The number of baffles reported is that on one half of the cylinder. No baffles were located at the symmetry plan.

2. Mathematical analysis

The steady-state equations for 2D laminar natural convection over a cylinder, including the Boussinesq approximation, are given by:

$$\frac{1}{r}\frac{\partial(ru)}{\partial r} + \frac{1}{r}\frac{\partial v}{\partial\theta} = 0 \tag{1}$$

$$u\frac{\partial u}{\partial r} + \frac{v}{r}\frac{\partial u}{\partial\theta} - \frac{v^2}{r} = \frac{1}{\rho}\left[\rho g\beta(T - T_\infty)\sin(\theta) - \frac{\partial p}{\partial r}\right] + \nu\left[\frac{\partial^2 u}{\partial r^2} + \frac{1}{r}\frac{\partial u}{\partial r} - \frac{u}{r^2} + \frac{1}{r^2}\frac{\partial^2 u}{\partial\theta^2} - \frac{2}{r^2}\frac{\partial v}{\partial\theta}\right] \tag{2}$$

$$u\frac{\partial v}{\partial r} + \frac{v}{r}\frac{\partial v}{\partial\theta} + \frac{uv}{r}$$

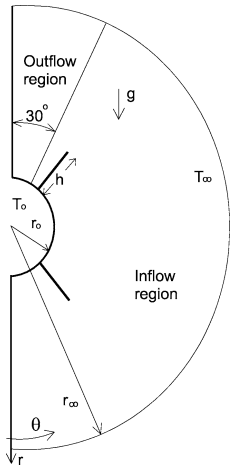

Fig. 1. Schematic of the problem, showing a case with non-uniform baffle distribution.

$$= \frac{1}{\rho}\left[\rho g\beta(T - T_\infty)\cos(\theta) - \frac{1}{r}\frac{\partial p}{\partial \theta}\right] + \nu\left[\frac{\partial^2 v}{\partial r^2} + \frac{1}{r}\frac{\partial v}{\partial r} - \frac{v}{r^2} + \frac{1}{r^2}\frac{\partial^2 v}{\partial \theta^2} + \frac{2}{r^2}\frac{\partial u}{\partial \theta}\right] \quad (3)$$

$$u\frac{\partial T}{\partial r} + \frac{v}{r}\frac{\partial T}{\partial \theta} = \alpha\nabla^2 T \quad (4)$$

where,

$$\nabla^2 \equiv \left[\frac{\partial^2}{\partial r^2} + \frac{1}{r}\frac{\partial}{\partial r} + \frac{1}{r^2}\frac{\partial^2}{\partial \theta^2}\right]$$

Eqs. (1)–(4) are subject to the following boundary conditions:

(1) On the cylinder surface, i.e., $r = r_o$; $u = v = 0$ and $T = T_o$.
(2) Far-stream from the cylinder, i.e., $r \to \infty$; $\partial v/\partial r = 0$. As for the temperature, and following the work of Kuehn and Goldstein [3] and Abu-Hijleh et al. [8], the far-stream boundary condition is divided into an inflow ($\theta \leqslant 150$ degrees) and an outflow ($\theta > 150$ degrees) regions, Fig. 1. The far-stream temperature boundary conditions are $T = T_\infty$ and $\partial T/\partial r = 0$ for the inflow and outflow regions, respectively.
(3) Plane of symmetry; $\theta = 0$ and $\theta = 180$ degrees; $v = 0$ and $\partial u/\partial\theta = \partial T/\partial\theta = 0$.
(4) On the baffle surface; $u = v = 0$. Since the baffles are assumed to be very thin and of very low conductivity, there will be no heat conduction along the baffles. Thus, the temperature at any point along the baffle will be the average temperature of the fluid just above and just below the baffle, i.e., $T_{ij} = (T_{ij+1} + T_{ij-1})/2$, see Fig. 2.

The local and average Nusselt numbers, based on cylinder diameter, are calculated as:

$$Nu_{D,s} = \frac{Dh(\theta)}{k};$$

$$\overline{Nu_D} = \frac{1}{\pi}\frac{D}{k}\int_0^\pi h(\theta)\,d\theta = -\frac{D}{\pi}\int_0^\pi \frac{\partial T(r_o,\theta)/\partial r}{T_o - T_\infty}\partial\theta \quad (5)$$

The following non-dimensional groups are introduced:

$$R \equiv \frac{r}{r_o}, \qquad U \equiv \frac{ur_o}{\alpha}, \qquad V \equiv \frac{vr_o}{\alpha},$$
$$\phi \equiv \frac{T - T_\infty}{T_o - T_\infty}, \qquad P \equiv \frac{p - p_\infty}{\rho\alpha^2/r_o^2} \quad (6)$$

Using the steam function—vorticity formulation, the non-dimensional form of Eqs. (1)–(4) is given by:

$$\omega = \nabla^2\psi \quad (7)$$

$$U\frac{\partial\omega}{\partial R} + \frac{V}{R}\frac{\partial\omega}{\partial\theta} = Pr\nabla^2\omega + Ra\,Pr\left[\sin\theta\frac{\partial\phi}{\partial R} + \frac{\cos(\theta)}{R}\frac{\partial\phi}{\partial\theta}\right] \quad (8)$$

$$U\frac{\partial\phi}{\partial R} + \frac{V}{R}\frac{\partial\phi}{\partial\theta} = \nabla^2\phi \quad (9)$$

where,

$$U \equiv \frac{1}{R}\frac{\partial\psi}{\partial\theta}, \qquad V \equiv -\frac{\partial\psi}{\partial R}, \qquad Ra = \frac{g\beta r_o^3(T_o - T_\infty)}{\alpha\nu},$$
$$Ra_D = \frac{g\beta D^3(T_o - T_\infty)}{\alpha\nu}, \qquad Pr = \frac{\nu}{\alpha} \quad (10)$$

The new non-dimensional boundary conditions for Eqs. (7)–(9) are given by:

(1) On the cylinder surface, i.e., $R = 1.0$; $\psi = \partial\psi/\partial R = 0$, $\omega = \partial^2\psi/\partial R^2$, and $\phi = 1.0$.
(2) Far-stream form the cylinder, i.e., $R \to \infty$; $\partial^2\psi/\partial R^2 = 0$ and $\omega = (1/R^2)(\partial^2\psi/\partial\theta^2)$. For the non-dimensional temperature, $\phi = 0$ and $\partial\phi/\partial R = 0$, for the inflow and outflow regions, respectively.
(3) Plane of symmetry; $\psi = \omega = \partial\phi/\partial\theta = 0$.
(4) On the baffle surface; $\psi = 0$, $\omega = (1/R^2)(\partial^2\psi/\partial\theta^2)$, and $\phi_{ij} = (\phi_{ij+1} + \phi_{ij-1})/2$.

The reduction in the convection heat transfer from the cylinder due to the addition of the baffle(s) is presented in terms of the normalized Nusselt number ($\overline{NU_{D,B}}$) and the percentage baffle "cost-efficiency" (η_{Bc}), as per Eqs. (11) and (12) below. The first term shows the relative reduction in the Nusselt number while the second shows the percentage relative reduction in the Nusselt number per unit length of baffle(s) used. The percentage baffle "cost-efficiency" should not be confused with the standard definition of fin efficiency or effectiveness. This parameter gives an idea about the economic return of using the baffle(s).

$$\overline{NU_{D,B}} = \frac{\overline{Nu_{D,B}}}{\overline{Nu_{D,o}}} \quad (11)$$

$$\eta_{Bc}(\%) = \frac{1 - \overline{NU_{D,B}}}{B * H} * 100 \quad (12)$$

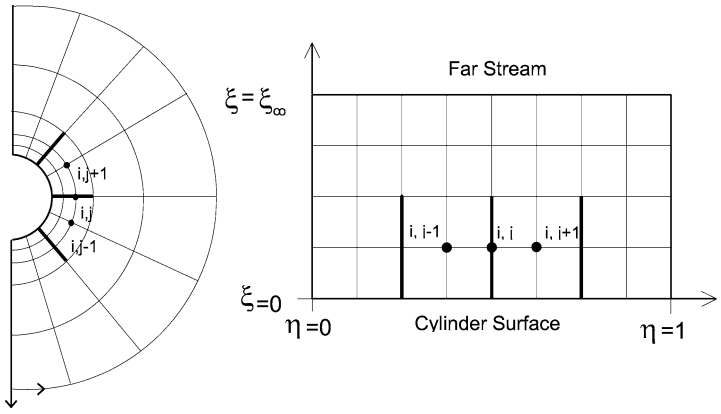

Fig. 2. Schematic of the computational grid in the physical (left) and computational (right) domains, showing a case with uniform baffle distribution.

In order to accurately resolve the boundary layer around cylinder, a grid with small radial spacing is required. It is not practical to use this small spacing as we move to the far-stream boundary. Thus a stretched grid in the radial direction is needed [15]. This will result in unequally spaced nodes and would require the use of more complicated and/or less accurate finite difference formulas. To overcome this problem, the unequally spaced grid in the physical domain (R, θ) is transformed into an equally spaced grid in the computational domain (ξ, η) [15], Fig. 2. The two domains are related as follows:

$$R = e^{\pi\xi}, \qquad \theta = \pi\eta \tag{13}$$

Eqs. (7)–(9) along with the corresponding boundary conditions need to be transformed into the computational domain. In the new computational domain, the current problem is given by:

$$\omega = \frac{1}{E^2}\left[\frac{\partial^2\psi}{\partial\xi^2} + \frac{\partial^2\psi}{\partial\eta^2}\right] \tag{14}$$

$$\frac{\partial^2\omega}{\partial\xi^2} + \frac{\partial^2\omega}{\partial\eta^2} = \frac{1}{Pr}\left[\frac{\partial\psi}{\partial\eta}\frac{\partial\omega}{\partial\xi} - \frac{\partial\psi}{\partial\xi}\frac{\partial\omega}{\partial\eta}\right] - ERa\left[\sin(\pi\eta)\frac{\partial\phi}{\partial\xi} + \cos(\pi\eta)\frac{\partial\phi}{\partial\eta}\right] \tag{15}$$

$$\frac{\partial^2\phi}{\partial\xi^2} + \frac{\partial^2\phi}{\partial\eta^2} = \left[\frac{\partial\psi}{\partial\eta}\frac{\partial\phi}{\partial\xi} - \frac{\partial\psi}{\partial\xi}\frac{\partial\phi}{\partial\eta}\right] \tag{16}$$

where,

$$E = \pi e^{\pi\xi} \tag{17}$$

The transformed boundary conditions are given by:

(1) On the cylinder surface, i.e., $\xi = 0$; $\psi = \partial\psi/\partial\xi = 0$, $\omega = (1/\pi^2)(\partial^2\psi/\partial\xi^2)$, and $\phi = 1.0$.
(2) Far-stream form the cylinder, i.e., $\xi \to \infty$; $\partial^2\psi/\partial\xi^2 = 0$ and $\omega = (1/E^2)(\partial^2\psi/\partial\eta^2)$. For the non-dimensional temperature $\phi = 0$ and $\partial\phi/\partial\xi = 0$, for the inflow and outflow regions, respectively.
(3) Plane of symmetry; i.e., $\eta = 0$ and $\eta = 1$; $\psi = \omega = \partial\phi/\partial\eta = 0$.
(4) On the baffle surface; $\psi = 0, \omega = (1/E^2)(\partial^2\psi/\partial\eta^2)$, and $\phi_{ij} = (\phi_{ij+1} + \phi_{ij-1})/2$.

The system of elliptic PDEs given by Eqs. (14)–(16) along with the corresponding boundary conditions was discretized using the finite difference method. The resulting system of algebraic equations was solved using the hybrid scheme [16]. Such a method proved to be numerically stable for convection–diffusion problems. The finite difference form of the equations was checked for consistency with the original PDEs [16]. The iterative solution procedure was carried out until the error in all solution variables (ψ, ω, ϕ) became less than a predefined error level (ε). Other predefined parameters needed for the solution method included the placement of the far-stream boundary condition (R_∞) and the number of grid points in both radial and tangential directions, N and M, respectively. Extensive testing was carried out in order to determine the effect of each of these parameters on the solution. This was done to insure that the solution obtained was independent of and not tainted by the predefined value of each of these parameters. The testing included varying the value of ε from 10^{-3} to 10^{-6}, R_∞ from 5 to 50, N from 100 to 200, and M from 60 to 144.

In the previous work of uniformly spaced baffles [11], the number of grid points was varied in the radial ($N = 133$–141) and tangential ($M = 117$–120) directions in order to insure that all baffles coincided with one of the grid's radial lines and that the baffle's end coincided with one of the grid's tangential lines, see Fig. 2. The need for the baffles to coincide with the grid was also observed in this study but in a different fashion. In order to avoid any changes that might result from using different grids for different combinations of number baffle(s) and baffle height, a fixed size grid was used for all combinations in this study ($N = 160 \times M = 120$). In this study the baffle's tangential location was varied in 15 degrees increments between 15–165 degrees. Thus using $M = 120$ insured that the tangential grid resolution was suitable for all tangential baffle locations. The hardest part was adjusting the radial grid resolution to insure that the baffle's end coincided with one of the radial grid points.

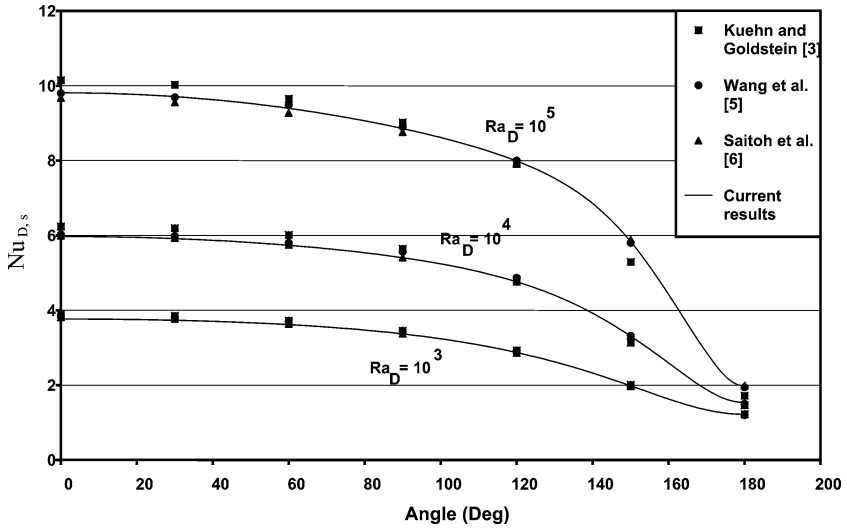

Fig. 3. Comparison of the local Nusselt number for the case of a cylinder without baffles.

In this study the nominal baffle heights (H) used were: 0.1, 0.25, 0.5, 1.0, and 1.5. The combination of $N = 160$ and $R_\infty = 13.0$ resulted in a difference of less than 1% between the actual baffle height and the nominal baffle height used in the current study. The actual height being that of the baffle used in the calculation with its end coinciding with the closest radial grid point while using a fixed radial grid resolution ($N = 160$). The accuracy of the local Nusselt number calculations, $Nu_{D,s}(\theta)$, is another measure of the accuracy of the numerical code. Fig. 3 shows very good agreement between the profiles of the local Nusselt number calculated by the current code and the data reported by Kuehn and Goldstein [3], Wang et al. [5], and Saitoh et al. [6], for the case of cylinder with no baffles. The results reported herein are based on the following combination: $N = 160$, $M = 120$, $R_\infty = 13.0$, and $\varepsilon = 10^{-5}$.

The non-dimensional form of the local entropy generation equation in 2D cylindrical coordinates can be written as [12]:

$$S''_{\text{gen}} = \frac{1}{(\phi + \overline{T})^2}\left[\left(\frac{\partial \phi}{\partial R}\right)^2 + \left(\frac{1}{R}\frac{\partial \phi}{\partial \theta}\right)^2\right] + \frac{\sigma}{(\phi + \overline{T})}\left\{2\left[\left(\frac{\partial U}{\partial R}\right)^2 + \frac{1}{R^2}\left(\frac{\partial V}{\partial \theta} + U\right)^2\right] + \left[\frac{1}{R}\frac{\partial U}{\partial \theta} + R\frac{\partial}{\partial R}\left(\frac{V}{R}\right)\right]^2\right\} \tag{18}$$

where

$$\overline{T} = \frac{T_\infty}{T_\text{o} - T_\infty}, \qquad \sigma = \frac{\alpha^2 \mu}{r_\text{o}^2 k (T_\text{o} - T_\infty)} \quad \text{and}$$

$$S''_{\text{gen}} = \frac{s''_{\text{gen}} r_\text{o}^2}{k} \tag{19}$$

The total non-dimensional entropy generation is calculated by integrating S''_{gen} over the entire flow filed:

$$N_\text{s} = \int_1^{R_\infty} \int_0^{\pi} S''_{\text{gen}}(R, \theta)\, \mathrm{d}\theta\, \mathrm{d}R \tag{20}$$

The range of N_s is very large, thus the logarithm to base ten is usually used, $\log(N_\text{s})$ [12]. There are two components in the entropy generation equation: the conduction part and the viscous dissipation part, the first and second terms on the right-hand side of Eq. (18), respectively. The values of the local and total entropy generation were calculated after the velocity and temperature profiles were obtained from the numerical iterations. Thus there was no need to transform Eq. (18) into the computational domain.

3. Results

The effect of baffles on the natural heat transfer from a horizontal isothermal cylinder was studied for several combinations of uniformly space baffle ($B = 1, 2, 3, 5, 11$) as well as a single and dual baffle(s) configuration with different baffle(s) tangential locations. The tangential location of the single or dual baffle(s) was changed from 15 to 165 degrees in 15 degrees increments, see Figs. 1 and 2. The uniform spacing cases served as a reference against which the effectiveness of the variable tangential location will be measured. Other parameters changed included the non-dimensional baffle height ($H = 0.1, 0.25, 0.5, 1.0, 1.5$) and Rayleigh number ($Ra = 10^3, 10^4, 10^5$). Eq. (18) introduces a new parameter in the calculation of entropy generation. The cylinder size has a direct effect on the entropy generation even for the same values of Rayleigh number, number of baffles, and baffle height. Entropy generation was calculated for several cylinder diameters ($D = 10^{-3}, 10^{-2}, 0.1, 1.0, 10.0$ m) at every combination of

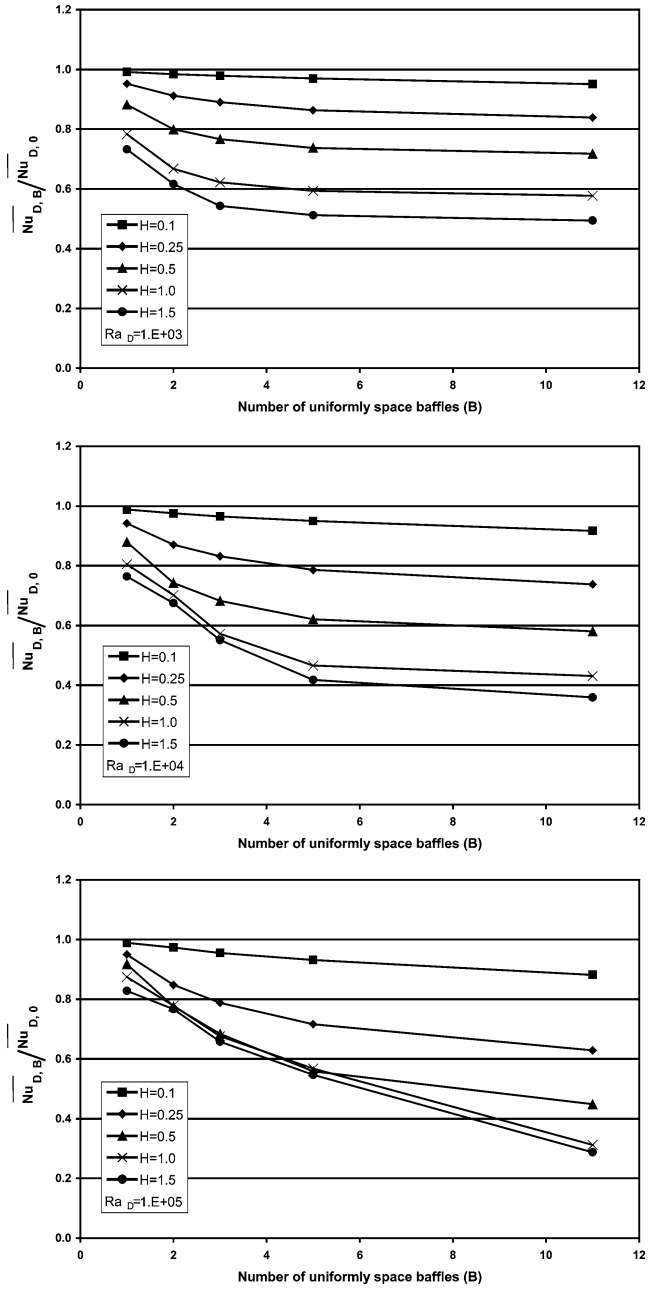

Fig. 4. Change in the normalized Nusselt number using uniformly spaced baffles.

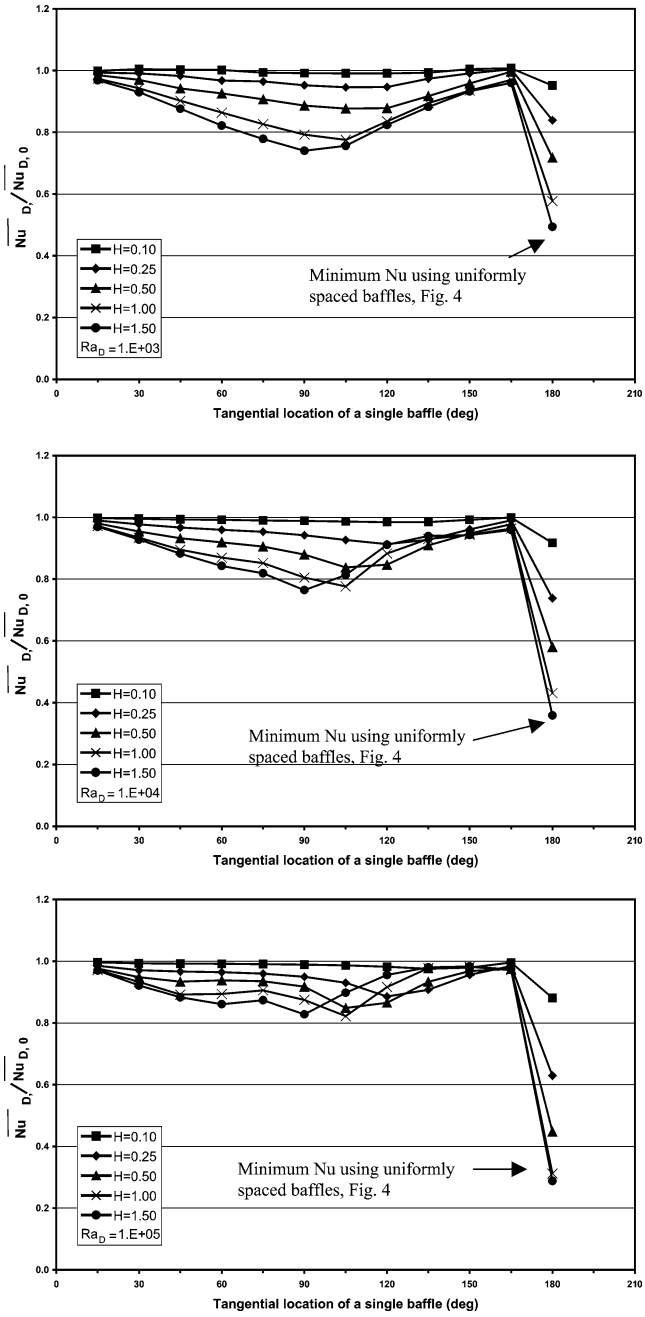

Fig. 5. Change in the normalized Nusselt number using a single baffle at different tangential locations.

Rayleigh number, number of baffles, baffle tangential location, and baffle height.

Fig. 4 shows the change in the normalized Nusselt number as a function of number of uniformly spaced baffles and baffle height for different values of Rayleigh number. There was up to 74% reduction in the value of normalized Nusselt number, depending on the number and height of baffles as well as the Rayleigh number. At low Rayleigh number, there seems to be an optimal number of baffles for a given baffle height beyond which further increases in the number of baffles had little effect on the normalized Nusselt number. Such data can be used to optimize the thermal insulation design of baffle equipped cylinders. As the Rayleigh number increased, the optimal number of baffles increased. For $Ra_D = 10^5$, the normalized Nusselt number continued to decrease as the number of baffles increased. Thus, there was no optimal number of baffles for $Ra_D = 10^5$, at least not for the number of baffles considered in this study. In all cases, the minimum normalized Nusselt number was achieved at $B = 11$. This value will be used in the following figures to asses the effectiveness of varying the tangential location of a single or dual baffle(s) configuration.

Fig. 5 shows the change in the normalized Nusselt number when using a single baffle as a function of the baffle's tangential location. The minimum normalized Nusselt number achieved using uniform baffles is shown at tangential location $\theta = 180$ degrees. From this figure it can be noted that the optimal tangential location of a single baffle is between 90–120 degrees, depending on the baffle height and Rayleigh number. At these tangential locations, the baffle is most effective as it strongly dampens the buoyancy driven convection currents over the cylinder surface. It is interesting to note that at low Rayleigh number, a properly placed baffle reduces the normalized Nusselt number by 50% compared to the use of 11 baffles ($Ra_D = 10^3$ and $H \geqslant 0.5$). The effectiveness of a single baffle is less at higher Rayleigh num-

Table 1
Optimal tangential location of a single baffle from minimum $\overline{NU}_{D,B}$

Rayleigh number (Ra_D)	Baffle height (H)				
	$H = 0.10$	$H = 0.25$	$H = 0.50$	$H = 1.00$	$H = 1.50$
10^3	120	120	120	105	90
10^4	120	120	105	105	90
10^5	135	120	105	105	90

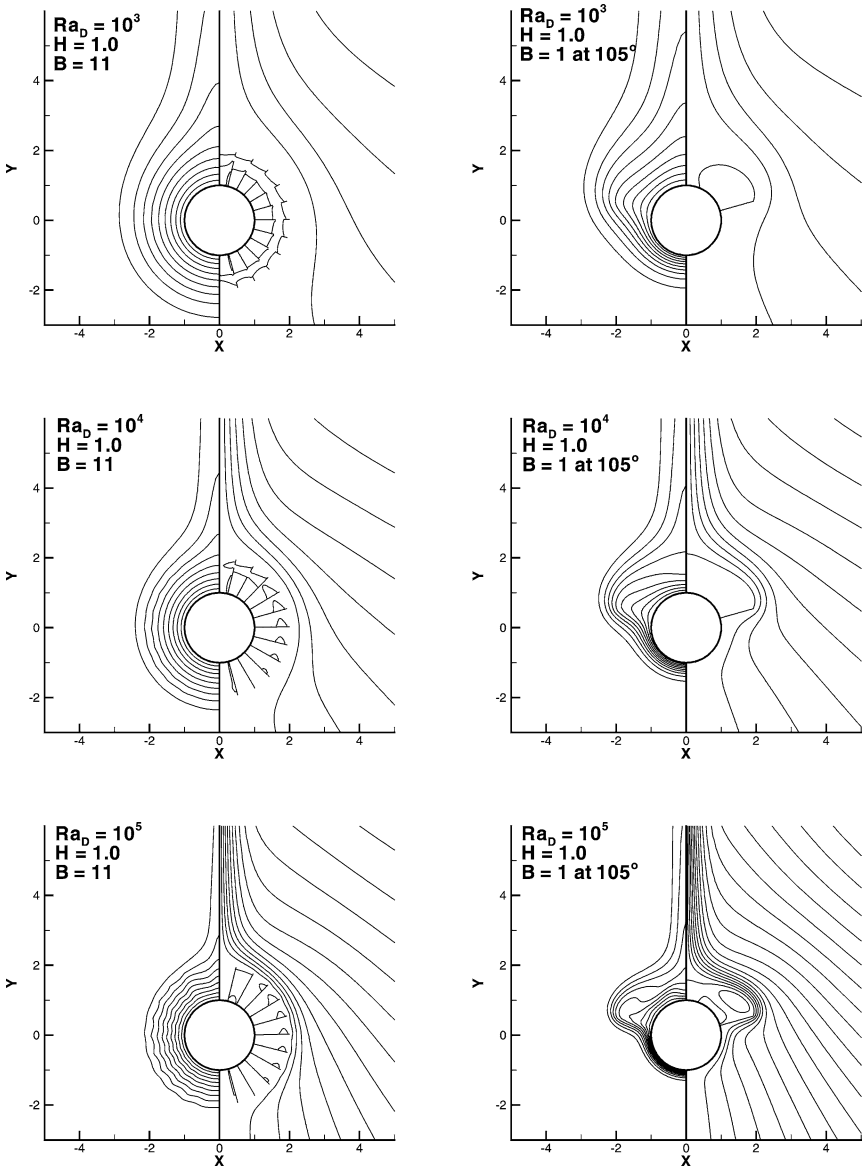

Fig. 6. Streamlines (right) and isotherms (left) comparing selective cases of maximum number of uniform baffles ($B = 11$) with the corresponding optimal single baffle ($B = 1$).

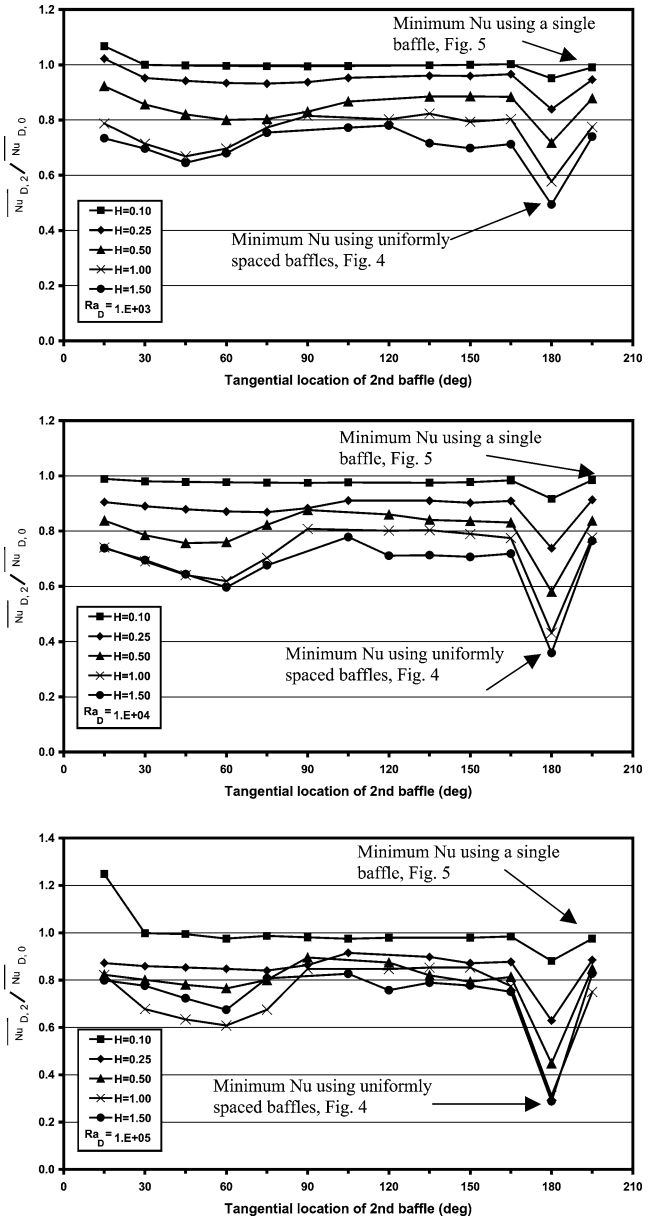

Fig. 7. Change in the normalized Nusselt number using two baffles, one fixed at the optimal position and the second at different tangential locations.

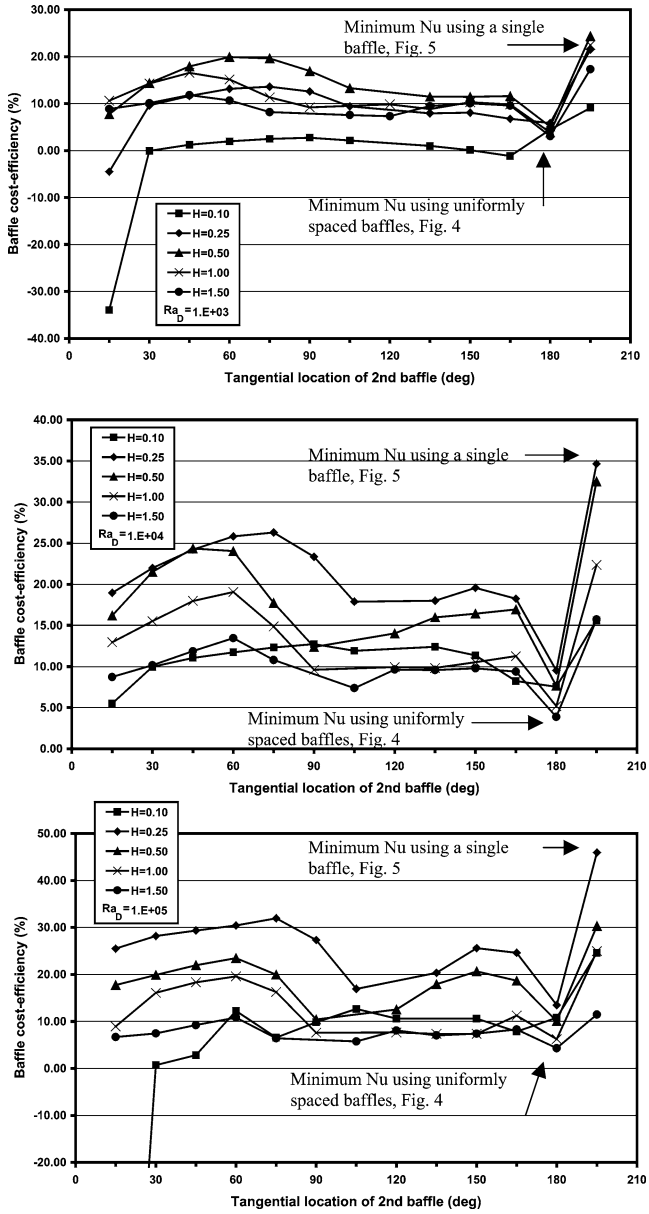

Fig. 8. Change in the baffle cost-efficiency using two baffles, one fixed at the optimal position and the second at different tangential locations.

bers. At low Ra_D the convection currents are weak and the presence of a single baffle is enough to result in a significant reduction in the convection currents. This is not the case at high Ra_D. Fig. 6 shows the streamlines and isotherms for the case of uniformly spaced baffles ($B = 11$) and an optimally positioned single baffle for the different values of Rayleigh number studied. Table 1 shows the optimal tangential location of a single baffle for all combinations of Rayleigh number and baffle height.

Fig. 7 shows the change in the normalized Nusselt number when using two baffles as a function of the second baffle's tangential location. The first baffle is fixed at the optimal location listed in Table 1. The minimum normalized Nusselt number achieved using uniform baffles is shown at tangential location $\theta = 180°$ while the minimum normalized Nusselt number achieved using a single baffle is shown at tangential location $\theta = 195°$. From this figure it can be noted that the optimal tangential location of the second baffle is between 45–60°, depending on the baffle height and Rayleigh number. It is clear that an improper placement of the second baffle may not lead to any further reduction in the normalized Nusselt number or even be counterproductive in causing a slight increase in $\overline{NU}_{D,B}$ from the case of an optimized single baffle. This clearly shows the importance of proper baffle placement based on the overall changes to the flow field. This also raises the issue of baffle percentage "cost-efficiency" (η_{Bc}). Fig. 8 shows change in η_{Bc} when using two baffles as a function of the second baffle's

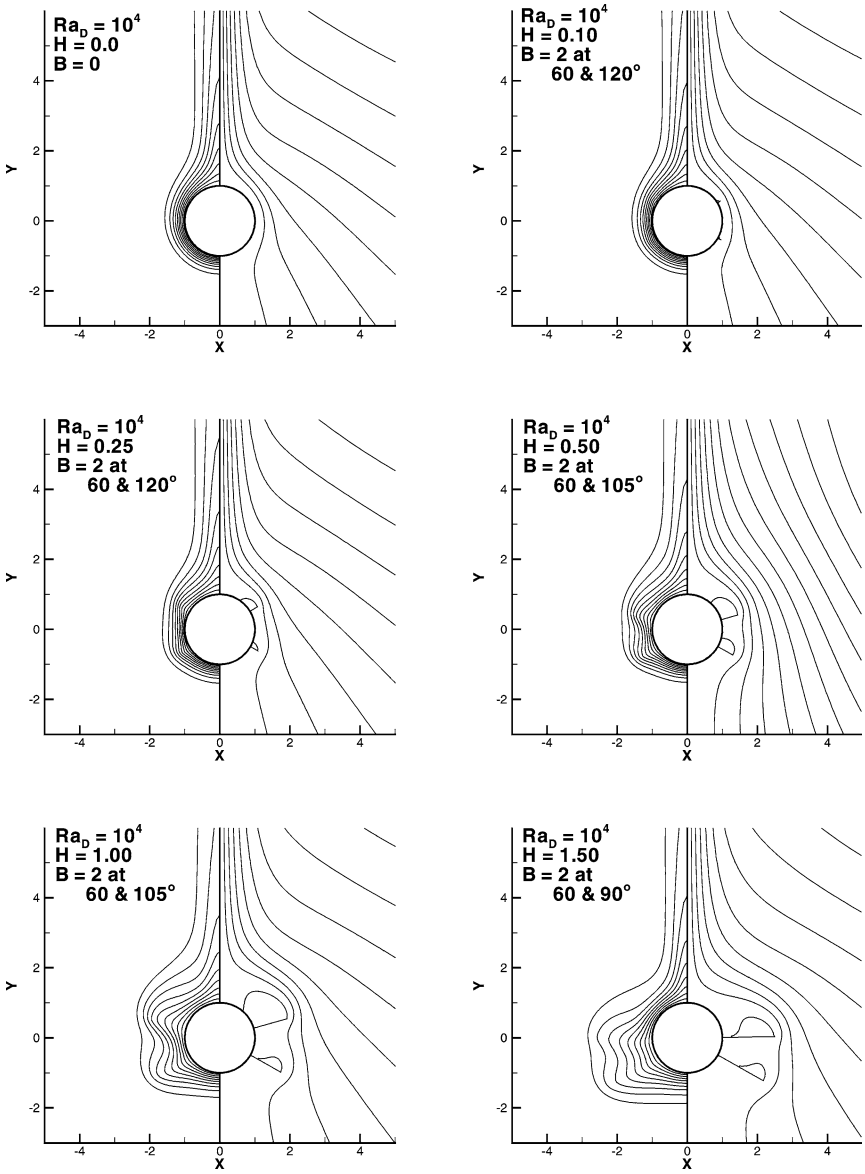

Fig. 9. Streamlines (right) and isotherms (left) at different baffle heights for the configurations of optimal two baffle tangential placement ($B = 2$).

tangential location. As in Fig. 7, η_{Bc} achieved using uniform baffles is shown at tangential location $\theta = 180°$ while η_{Bc} achieved using a single baffle is shown at tangential location $\theta = 195°$. From this figure it is clear that a properly placed single baffle has the maximum "cost-efficiency" and only a properly placed second baffle can have a "cost-efficiency" close to that of the single baffle. The "cost-efficiency" is highest for baffle heights in the range of 0.25–0.50. This baffle height spans most of the buoyancy deriver convection thermal boundary that forms around the cylinder thus having the most tempering effect on the heat transfer from the cylinder. This can be seen from Fig. 9 which includes selective streamlines and isotherms for different baffles' locations and heights at $Ra_D = 10^4$.

Fig. 10 shows sample graphs of the non-dimensional entropy generation, $\log(N_s)$, at different combinations of Rayleigh number and cylinder diameter. The value at $\theta = 0°$ corresponds to the entropy generation of a smooth cylinder, $B = 0$. The trend in $\log(N_s)$ is very similar to that of $\overline{NU}_{D,B}$ which suggests that entropy generation is dominated by thermal rather than viscous effects. The dominance of thermal versus viscous entropy generation in natural convection heat transfer from a horizontal cylinder was detailed in a previous work by the author [17]. The change in the cylinder diameter only lowered the value of entropy generation but had little effect on the trend. This suggests that using baffles also results in a more thermodynamically efficient system. The effect of using a single baffle at different tangential locations can be seen in Fig. 11. It is interesting to note that an optimized baffle is more effective in reducing the entropy generation at larger cylinder diameters. This can be traced to the parameter (σ) in the viscous entropy generation component in Eq. (18), the second term on the right. This term is inversely proportional

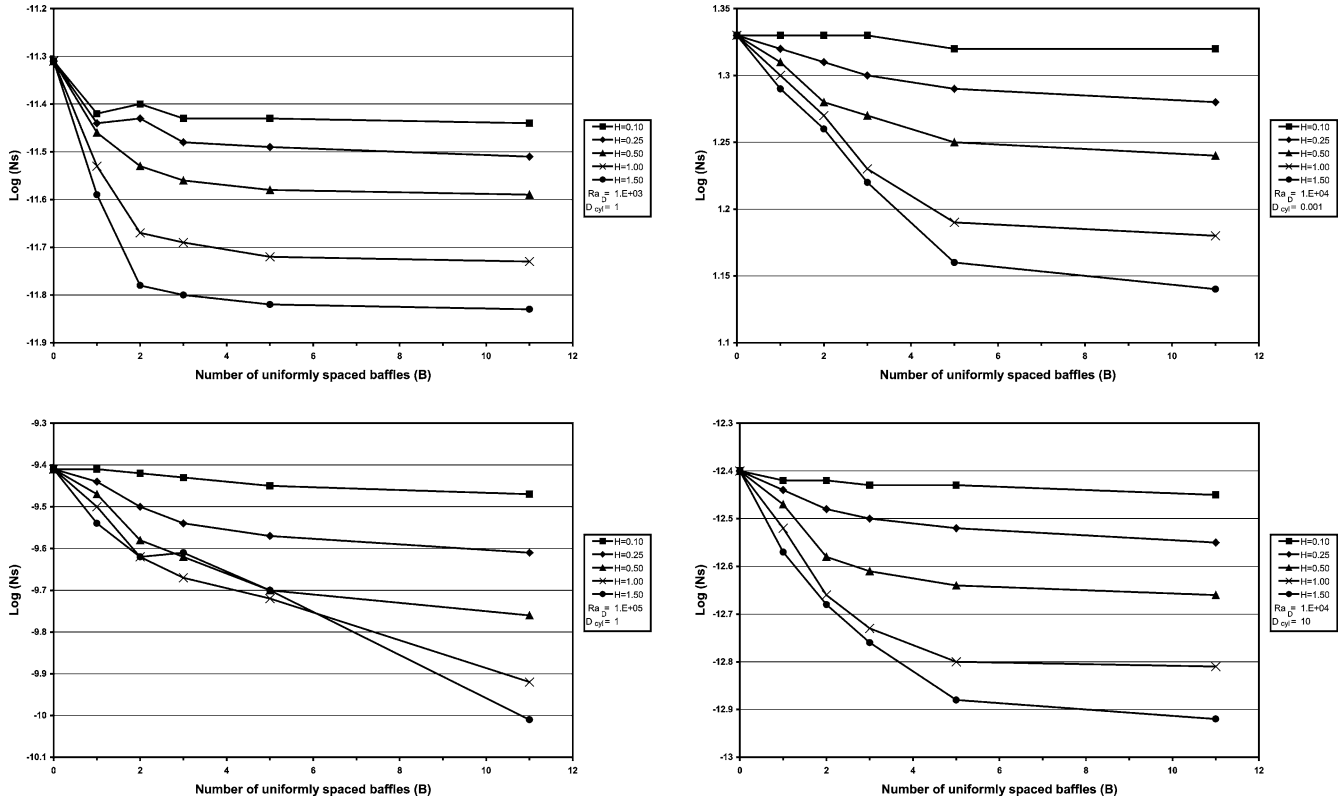

Fig. 10. Samples of the change in non-dimensional entropy generation using uniformly spaced baffles.

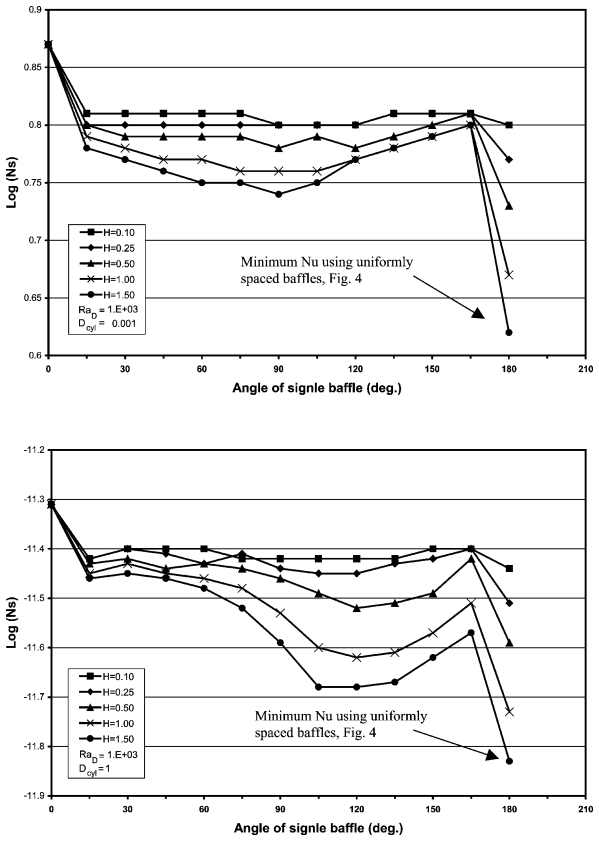

Fig. 11. Samples of the cylinder diameter effect on the non-dimensional entropy generation using a single baffle at different tangential locations.

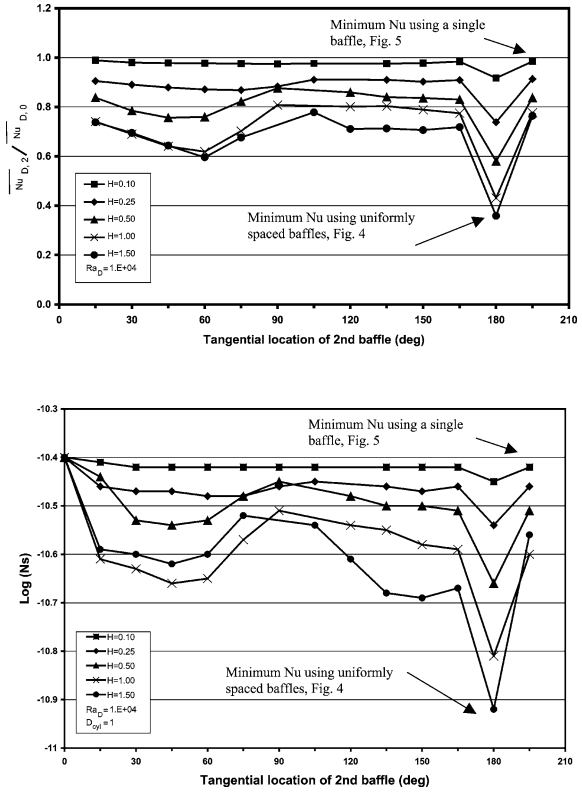

Fig. 12. Change in the normalized Nusselt number (top) and the non-dimensional entropy generation (bottom) at $Ra_D = 10^4$ using two baffles, one fixed at the optimal position and the second at different tangential locations.

to the cylinder radius while the thermal entropy generation component is not affected by the cylinder radius. This indicates that using baffles on large diameter cylinders is more effective in reducing entropy generation and thus enhancing the thermodynamic efficiency of the system. Fig. 12 shows sample entropy generation curves when using two baffles. The trend of $\log(N_s)$ is that of $\overline{NU}_{D,B}$ which confirms that the entropy generation is mainly due to thermal effects.

4. Conclusions

The problem of natural heat transfer from an isothermal horizontal cylinder with different configurations of low conductivity baffles was studied numerically. Changes in the average Nusselt number at different combinations of number of baffles, baffle height, baffle tangential location, and Rayleigh number were reported. The local velocity and temperature data were used to calculate the local and global entropy generation. Selective results of the changes in the total entropy generation due to the presence of the baffles and at difference cylinder diameters were presented and discussed. The results indicate that proper positioning of one or two baffles can reduce the heat transfer from the cylinder by as much as 70% compared to using 11 uniformly spaced baffles. This optimization of baffle placement has great design and economic implications. Baffles with a non-dimensional height of 0.25–0.50 had the highest "cost-efficiency". Entropy generation was greatly reduced by the use of baffles, which leads to more thermodynamically efficient systems. The baffles were more effective at reducing entropy generation when used on large diameter cylinders. Entropy generation was mainly due to thermal rather than viscous effects.

References

[1] V.T. Morgan, The overall convective heat transfer from smooth circular cylinders, Adv. Heat Transfer 11 (1975) 199–264.
[2] S.W. Churchill, H.H.S. Chu, Correlating equations for laminar and turbulent free convection from a horizontal cylinder, Internat. J. Heat Mass Transfer 18 (1975) 1049–1053.
[3] T.H. Kuehn, R.J. Goldstein, Numerical solutions to the Navier–Stockes equations for laminar natural convection about a horizontal cylinder, Int. J. Heat Mass Transfer 23 (1980) 971–979.
[4] B. Farouk, S.I. Guceri, Natural convection from a horizontal cylinder-laminar regime, J. Heat Transfer 103 (1981) 522–527.
[5] P. Wang, R. Kahawita, T.H. Nguyen, Numerical computation of the natural convection flow about a horizontal cylinder using splines, Numer. Heat Transfer Part A 17 (1990) 191–215.
[6] T. Saitoh, T. Sajik, K. Maruhara, Bench mark solutions to natural convection heat transfer problem around a horizontal circular cylinder, Internat. J. Heat Transfer 36 (1993) 1251–1259.
[7] J.C. Chai, S.V. Patankar, Laminar natural convection in internally finned horizontal annuli, Numer. Heat Transfer Part A 24 (1993) 67–87.
[8] B. A/K Abu-Hijleh, M. Abu-Qudais, E. Abu-Nada, Entropy generation due to laminar natural convection from a horizontal isothermal cylinder, J. Heat Transfer 120 (1998) 1089–1990.
[9] K. Vafai, P.C. Huang, Analysis of heat transfer regulation and modification employing intermittently emplaced porous cavities, J. Heat Transfer 116 (1994) 604–613.
[10] M.A. Al-Nimr, M.K. Alkam, A modified tubeless solar collector partially filled with porous substrate, Renewable Energy 13 (1998) 165–173.
[11] B. A/K Abu-Hijleh, Natural convection heat transfer and entropy generation from a cylinder with baffles, ASME J. Heat Transfer 122 (2000) 679–692.
[12] A. Bejan, Entropy Generation Through Heat and Fluid Flow, Wiley, New York, 1982.
[13] A.C. Baytas, Entropy generation for natural convection in an inclined porous cavity, Internat. J. Heat Mass Transfer 43 (2000) 2089–2099.
[14] A. Bejan, Shape and Structure, From Engineering to Nature, Cambridge University Press, Cambridge, 2000.
[15] J.D. Anderson, Computational Fluid Dynamics: The Basics with Applications, McGraw-Hill, New York, 1994.
[16] S.V. Patankar, Numerical Heat Transfer of Fluid Flow, McGraw-Hill, New York, 1980.
[17] B. A/K Abu-Hijleh, I.N. Jadallah, E. Abu Nada, Entropy generation due to natural convection from a horizontal isothermal cylinder in oil, Internat. Comm. Heat Mass Transfer 25 (1998) 1135–1143.